Effects of Morphology on Stability, Electronic, and Optical Properties of Rutile TiO2 Nanowires

ARTICLE *in* THE JOURNAL OF PHYSICAL CHEMISTRY C · NOVEMBER 2010

Impact Factor: 4.77 · DOI: 10.1021/jp106117y

Effects of Morphology on Stability, Electronic, and Optical Properties of Rutile TiO_2 Nanowires

D. B. Migas,*,† V. L. Shaposhnikov,† V. E. Borisenko,† and F. Arnaud D'Avitaya‡

Belarusian State University of Informatics and Radioelectronics, P.Browka 6, 220013 Minsk, Belarus and Centre Interdisciplinare de Nanoscience de Marseille CINAM UPR CNRS 3118 conventionée à Aix-Marseille Université Case 913, Campus de Luminy, 13288 Marseille Cedex 9, France

Received: July 2, 2010; Revised Manuscript Received: October 4, 2010

By means of first principles calculations we show that morphology of TiO_2 nanowires in the rutile phase turns out to be important in their stability and band gap engineering. The most stable ⟨001⟩-oriented TiO_2 nanowires are found to display the {110} facets while the most thermodynamically favorable nanowires with the ⟨110⟩ axis are characterized by the {110} and {001} facets. Our results clearly demonstrate that appearance of the {100} facets in the shape of TiO_2 nanowires in the ⟨001⟩ orientation leads to a sizable reduction of band gaps, however, it does not cause the shift of the absorption edge to the lower energy range. Presence of flat bands similar to localized band gap states in the gap region of the ⟨110⟩-oriented TiO_2 nanowires is predicted to be an intrinsic feature, which is not connected with O vacancies. We also discuss how our findings can be used for optimization of photovoltaic and photocatalytic cells.

Introduction

Titanium dioxide (TiO_2) displaying perfect chemical stability and oxidative ability can be considered as the most investigated material among metal oxides because it is used in a wide range of applications[1,2] including photocatalysis and photovoltaics. TiO_2 is characterized by the band gap of 3.0 (the rutile phase) and 3.2 eV (the anatase phase) indicating that only a small fraction of the sun's energy (mainly ultraviolet region) will be utilized in solar energy conversion and water splitting processes. To absorb visible light TiO_2 is usually doped or sensitized.[2] Another way to improve efficiency of photocatalytic and photovoltaic cells is to employ nanostructured TiO_2 because of its higher surface-to-volume ratio.[2]

Nanostructured TiO_2 in the form of nanowires (NWs) has recently attracted much attention because of its prospects for different applications such as humidity sensors,[3] photovoltaic[4] and photocatalytic[5] cells, optical devices,[6] and field-effect transistors.[7] Two approaches are usually used to produce TiO_2 NWs.[2] The first one called 'wet-chemistry' methods provides TiO_2 NWs in the anatase phase that are usually contaminated and the postgrown heat treatment is necessary to improve the crystallinity of these nanostructures. The latter issue also prevents straightforward integration of such NWs into semiconductor device fabrication. On the contrary, the 'dry' methods avoid these restrictions and high-quality TiO_2 NWs can be grown. In fact, TiO_2 NWs in the rutile phase are obtained by thermal evaporation[5,8−11] via vapor−liquid−solid and vapor−solid growth mechanisms, using Ni or Au as a catalyst, and by chemical vapor deposition.[7,12] Such TiO_2 NWs are found to be single crystalline with diameters of 10−100 nm and to have the ⟨110⟩[5,7−11] and ⟨001⟩[12] growth orientations. Very recently Peng and Li[13] published results of their first-principles calculations indicating an increase in band gap values due to quantum confinement effects of hydrogenated rutile TiO_2 NWs with the ⟨001⟩ orientation. Unfortunately, there is no either experimental or theoretical study which systematically and in detail addresses electronic and optical properties of nonhydrogenated rutile TiO_2 NWs with respect to their morphology, diameter, and growth axis. In this paper, by means of ab initio calculations, we shed some light on these issues.

Morphology of TiO_2 Nanowires

TiO_2 bulk in the rutile phase has the tetragonal structure (space group $P4_2/mmm$)[1] with the lattice parameters a_{bulk} = 4.584 Å and c_{bulk} = 2.953 Å. The unit cell contains 2 Ti and 4 O atoms. The first and the second coordination shells around each Ti atom comprise 4 and 2 O atoms, respectively.

The Wulff construction is considered to be useful in predicting the shape of a nanostructure that facets display low surface energies. In the case of TiO_2 in the rutile phase, the (110) surface has been shown to possess the lowest surface energy, followed by the (100), (011), and (001) surfaces, respectively.[14,15] For the ⟨001⟩-oriented TiO_2 NWs one can expect the {110} facets to characterize their surface (the rhomb case in Figure 1) and this morphology has been observed experimentally.[12] We have also investigated NWs in which the {110} and {100} facets are close in size (the polyhedron case in Figure 1) and where the {100} facets dominate with small in size {110} facets playing the role of edges (the square case in Figure 1). The unit cell parameter along the NWs axis ($a_{||}$) is equal to c_{bulk}.

In the case of TiO_2 NWs with axis along the ⟨110⟩ directions, the Wulff construction predicts the {110} and {001} facets to appear (the square case in Figure 1). Some other possible morphology can be the polyhedron (the {110}, {001}, and {112} facets are close in size) and the rhomb (only the {112} facets are present), which are also shown in Figure 1. Unfortunately, there is no information about the (112) surface and it is quite possible that such a surface is unstable as far as it has not been observed experimentally.[1,16,17] It should be mentioned here that the surface energies calculated in ref 14 are for ideal

* To whom correspondence should be addressed: E-mail: migas@mater.unimib.it.
† Belarusian State University of Informatics and Radioelectronics.
‡ CINAM.

10.1021/jp106117y
Published on Web 11/15/2010

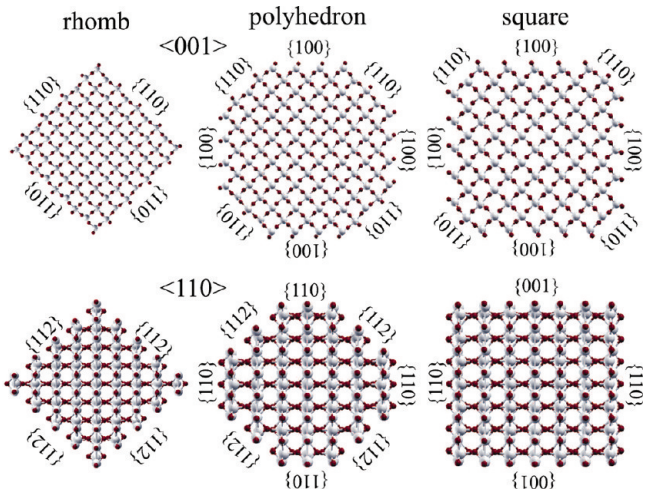

Figure 1. Cross sections of the ⟨001⟩-oriented TiO_2 NWs with diameters of about 3.9 nm (the top panel) and of the ⟨110⟩-oriented TiO_2 NWs with diameters of 2.9 nm (the bottom panel) displaying three possible morphology (the rhomb, the polyhedron, and the square), as optimized by USPP. The large, light-blue (gray) balls stand for Ti atoms, the small, red (dark) balls represent O atoms. All facets are indicated.

and infinite surfaces whereas a NW always displays the facet nature with edges. The latter issue indicates that the appearance of the facets, which are believed to be unstable, is not excluded especially if they act as edges.[18] For the ⟨110⟩-oriented TiO_2 NWs $a_{||}$ is assumed to be $a_{bulk}\sqrt{2}$. In addition, our structural models of TiO_2 NWs both with the ⟨001⟩ and the ⟨110⟩ axes do not have an O vacancy and they are characterized by the TiO_2 stoichiometry. Passivation by H is not necessary here because TiO_2 does not display the pure covalent nature of the chemical bonds. In the case of Si, where a sizable charge transfer between atoms is not expected due to the covalent bonds, any dangling bond remains at the surface and it can be saturated by H or by forming dimers. Instead of this the charge transfer in TiO_2 can "eliminate" a dangling bond at its surface since TiO_2 is characterized by a significant ionic contribution to the chemical bonds in addition to the possibility of O atoms to form double bonds. Moreover, in our structural models of TiO_2 NWs each O atom has two or three Ti atoms as the first neigbours and each Ti atom is surrounded at least by five O atoms, so that the H passivation is not essential.

Computational Details

The structural optimization and the band structure calculations for TiO_2 NWs have been performed by the first principles total-energy ultrasoft pseudopotentials (USPP) method (code VASP)[19−21] with plane-wave basis-set. Exchange and correlation potentials were included using the generalized gradient approximation (GGA) of Perdew and Wang.[22] Periodic boundary conditions were applied in the ⟨001⟩ or ⟨110⟩ direction. We have found that 7 Å of vacuum is enough to ensure a negligible interaction between neighboring NWs. This issue was checked by changing the vacuum thickness and monitoring variations in total energy. All atoms in TiO_2 NWs were allowed to relax. We set the energy cutoff at 300 eV. The grid of $1 \times 1 \times 6$ Monkhorst-Park points has been utilized in the calculations. The atomic relaxation was stopped when forces on the atoms were smaller than 0.05 eV/Å. To ensure convergence the final iterations have been performed on the $1 \times 1 \times 10$ grid. The optimization of $a_{||}$ was done by gradually increasing/decreasing its value along with the relaxation of the atomic positions until the equilibrium was reached. The calculations of band structures were performed on the self-consistent charge densities. In the case of the rutile TiO_2 bulk, the self-consistent procedure has been performed on the $8 \times 8 \times 16$ mesh. For some selected cases, we have used the projector-augmented wave method implemented in the VASP code and the GGA+U approach of Liechtenstein et al.[23] to take into account the on-site d−d Coulomb interaction. The cutoff value and the **k**-point mesh were kept the same as for USPP calculations. Total and projected DOS have been calculated by the tetrahedron method with Blöchl corrections.

The absorption coefficient was calculated by the full-potential linearized augmented plane wave method (WIEN2K package)[24] with the same generalized gradient approximation of Perdew and Wang.[22] The structural parameters of TiO_2 NWs fully optimized by the USPP method were used. The energy cutoff constant $R_{mt} \times K_{max} = 5.1$ and 6 **k**-points uniformly distributed in the irreducible part of the Brillouin zone were found to be sufficient for a self-consistent procedure. The dipole matrix element, which is the key ingredient for optical property calculations, has been evaluated at a dense grid of about 100 **k**-points in the irreducible part of the corresponding Brillouin zone. The effective mass tensors for holes and electrons were evaluated along the principal axes of the ellipsoidal energy surface in the band extrema by calculating the appropriate second derivatives within the five-point approximation.

Structural Optimization and Stability of TiO_2 Nanowires

The lattice parameters of the rutile TiO_2 bulk after the full structural relaxation are found to be $a_{bulk} = 4.630$ Å and $c_{bulk} = 2.981$ Å, which are close to the experimental values[1] and the other theoretical estimates.[15,25,26] In our case Ti−O bond lengths of the first and the second coordination shells in bulk are equal to 1.96 and 1.99 Å, respectively. The ⟨001⟩-oriented TiO_2 NWs regardless of morphology display 1.80−1.99 Å in Ti−O interatomic distances of the first coordination shell while the second coordination shell spans over 2.00−2.17 Å. The smallest Ti−O bond length of 1.80 Å involves the O bridging atoms on the surface of the {110} and {100} facets and this situation is commonly observed for the (110) and (100) surfaces.[16,27] TiO_2 NWs with the ⟨110⟩ axis show the smallest Ti−O interatomic distance of 1.75 Å on the surface of the {110} and {112} facets whereas variations in the bond lengths of the first and the second coordination shells are similar to those of the ⟨001⟩-oriented TiO_2 NWs. We have also found $a_{||}$ to be slightly shrunk with respect to the corresponding bulk values. Thus, the square TiO_2 NW with diameter of 2.0 nm possesses the largest (1%) deviation in $a_{||}$ among NWs with the ⟨001⟩ axis, while 2% is revealed for the rhomb TiO_2 NW with the ⟨110⟩ axis and diameter of 1.1 nm. An increase in diameter of NWs leads $a_{||}$ to be closer to the bulk values.

Figure 2a reports how total energy varies with respect to the number of formula units in the unit cell (also proportional to diameter) for TiO_2 NWs in the ⟨001⟩ orientation with different morphology. It is clearly seen that the rhomb morphology with the {110} facets (see Figure 1) is the most stable one in perfect agreement with the experimental observation.[12] The polyhedron morphology is slightly higher in energy while the square morphology turns out to be the least stable. In the case of the ⟨110⟩-oriented TiO_2 NWs the square morphology is thermodynamically preferable followed by the polyhedron and the rhomb ones, respectively, as can be seen in Figure 2b. Our results demonstrate that these dependences are not linear. In fact, for small diameter NWs a larger lowering in energy with increasing the number of formula units is evident with respect to large

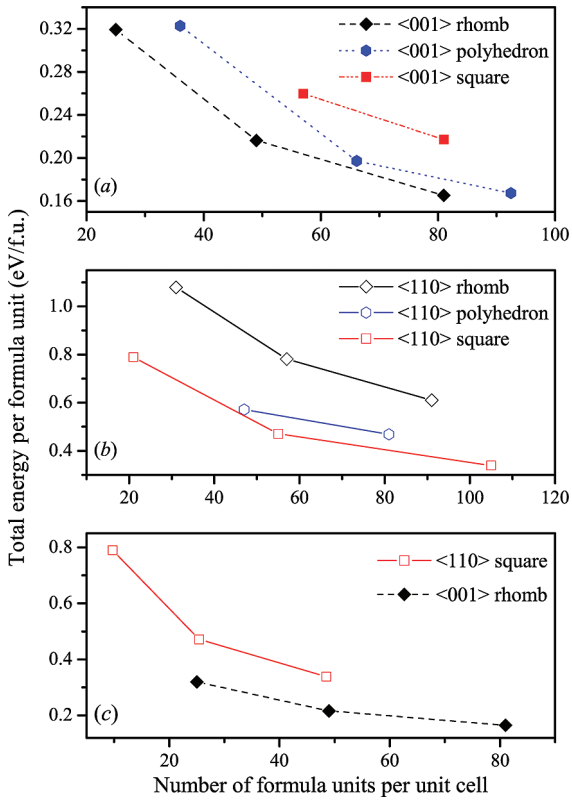

Figure 2. Dependences of total energy per formula unit on the number of formula units in the unit cell as calculated by USPP. (a) For the ⟨001⟩-oriented TiO_2 NWs with different morphology; (b) for the ⟨110⟩-oriented TiO_2 NWs with different morphology; (c) for the rhomb TiO_2 NWs with the ⟨001⟩ axis and the square TiO_2 NWs with the ⟨110⟩ axis. For comparison, the number of formula units per unit cell in the (c) section was rescaled to $a_{||} = c_{bulk}$ for the square TiO_2 NWs in the ⟨110⟩ orientation. Zero at the energy scale corresponds to energy of the TiO_2 formula unit in bulk of the rutile phase. The lines are a guide for the eye.

diameter NWs, while total energy per formula unit is closer to the bulk value for the latter NWs. This issue can be explained by a decrease in the surface-to-volume ratio and, as a consequence, the contribution to total energy from surface atoms is smaller than the one from bulk atoms. It also indicates that morphology is an important criterion determining stability of small diameter TiO_2 NWs, while for large diameter TiO_2 NWs its role is attenuated.

If we compare the most stable morphology of TiO_2 NWs in the ⟨001⟩ and ⟨110⟩ orientations, it is evident that the rhomb TiO_2 NWs with the ⟨001⟩ axis is thermodynamically favorable (see Figure 2c). This result was expected by considering the Wulff construction, as we pointed out in the previous section. However, the ⟨110⟩-oriented TiO_2 NWs are commonly observed[5,7−11] whereas there is only one paper[12] reporting the ⟨001⟩ orientation. We believe that the reasons for this issue are twofold. First of all, the largest TiO_2 NW considered in our paper has diameter no more than 4 nm while the smallest experimentally grown TiO_2 NWs are about 10 nm in diameter. As we have already stated, it is quite probable that the thermodynamic contribution to stability is independent of morphology if diameter of a TiO_2 NW is close or more than 10 nm. Second, for a TiO_2 NW to start growing, the system (a TiO_2 nucleation seed, the interface between a catalytic particle and a nucleation seed, and, if present, the interface between a substrate and a nucleation seed) should display low enough energy to surpass the nucleation barrier.[27,28] Thus, prevalence of the ⟨110⟩-oriented TiO_2 NWs can be attributed to more energetically preferable interfaces rather than to total energy of a nucleation seed. Similar effects have been revealed for silicon NWs.[18]

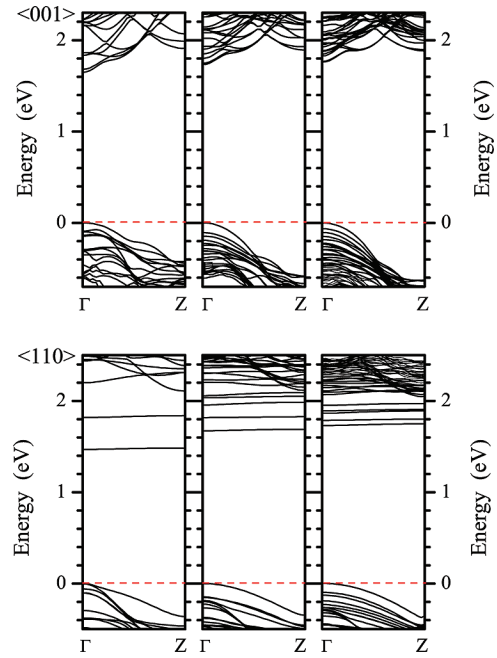

Figure 3. The band structures of TiO_2 NWs as calculated by USPP. (Top panel) The ⟨001⟩-oriented NWs with the rhomb morphology and diameters of 2.0, 2.9, and 3.9 nm, respectively from left to right; (Bottom panel) The ⟨110⟩-oriented NWs with the square morphology and diameters of 1.1, 2.0, and 2.9 nm, respectively, from left to right. Zero at the energy scale corresponds to the Fermi energy.

Band Structures and the Absorption Coefficient of TiO_2 Nanowires

The ⟨001⟩-oriented TiO_2 NWs with the rhomb morphology and the ⟨110⟩-oriented TiO_2 NWs with the square morphology have been shown to be thermodynamically stable and their band structures are presented in Figure 3. In the case of TiO_2 NWs with the ⟨001⟩ axis, we report the corresponding band diagrams for the nanostructures with diameters of 2.0, 2.9, and 3.9 nm, moving from left to right respectively (the top panel in Figure 3). It is clearly seen that band dispersion of such NWs near the gap region is almost the same displaying the direct nature of the gap in the Γ point. Here, one can expect a trend of decreasing the band gaps with increasing diameter of nanostructures caused by quantum confinement effects like in H-terminated TiO_2 NWs[13] and Si NWs.[29,30] However our results do not follow it indicating instead the gap values to be invariable and independent of diameter. We believe that presence of the states in the top valence bands and in the bottom conduction bands coming from atoms close to the surface is responsible for this issue. In fact, mainly the O-p states and the Ti-d states characterize the top valence bands and the bottom conduction bands, respectively, and they originate from all atoms including the ones close to and at the surface. On the contrary, the states of inner-core atoms dominate in the gap region in H-terminated TiO_2 NWs[13] and Si NWs[30] and the inner-core part of such NWs increases with diameter providing, in turn, the pronounced band gap reduction. The rather marginal blueshift of the band gap is experimentally observed for small anatase TiO_2 nanoparticles,[31,32] which is close to the error bar of the measurements,[31] and the effective mass model is shown to be not appropriate approximation to describe quantum size effects.[31,32] Thus, we can conclude

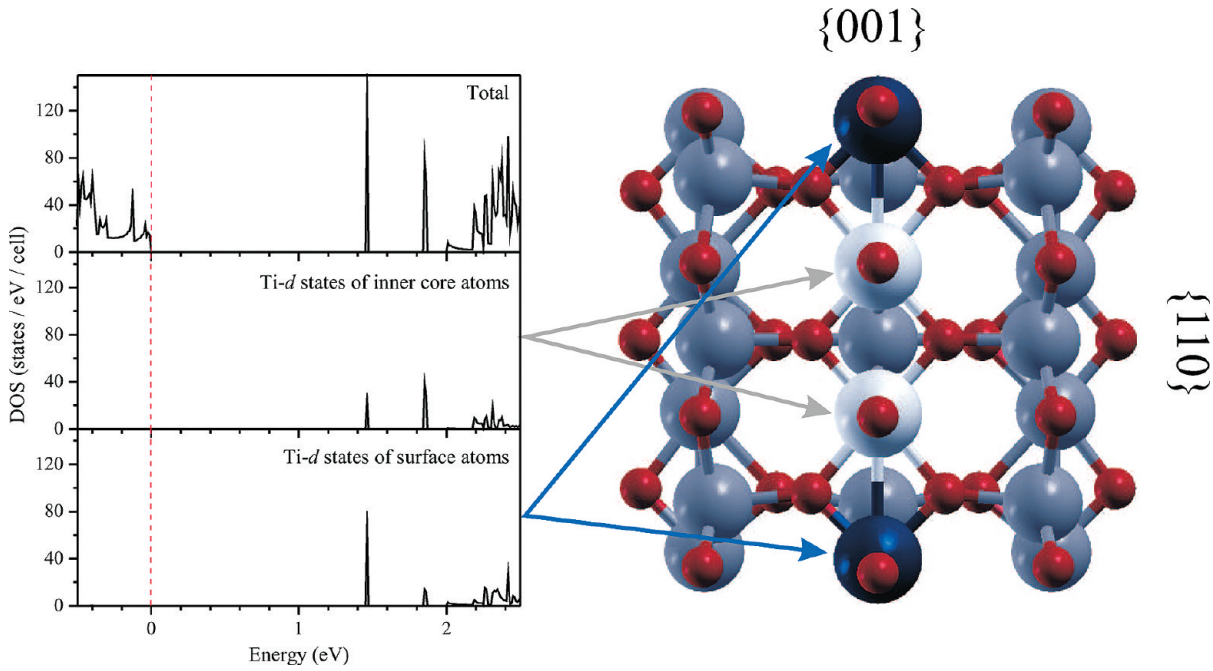

Figure 4. The total and projected density of states near the gap region (the left panel). Zero at the energy scale corresponds to the Fermi energy. Ti atoms, whose d states form localized bands in Figure 3, are indicated by arrows and by color in the cross section of the ⟨110⟩-oriented TiO_2 NW with the square morphology and diameter of 1.1 nm (the right panel). The small red (dark) balls represent O atoms. The large balls stand for Ti atoms.

that the states of the surface and close to the surface atoms in the top valence bands and in the bottom conduction bands stabilize the gaps in the ⟨001⟩-oriented TiO_2 NWs.

In the case of TiO_2 NWs with the ⟨110⟩ axis (the bottom panel in Figure 3), it is easy to trace similar features in the band structures described for the ⟨001⟩-oriented TiO_2 NWs. However, presence of the flat and separate bands in the bottom of the conduction band is evident. These flat bands look like band gap states and their number increases with diameter of NWs. Such localized band gap states are observed on the rutile (110) surface with O surface vacancies and attributed to the 3d orbitals of Ti^{3+} ions.[1] We have analyzed the character of the states of these flat bands and found out its Ti-d nature. In the case of the TiO_2 NW with a diameter of 1.1 nm, the Ti atoms providing the main contribution to these states are indicated in Figure 4. Only two of them stay on the (001) surface, but not on the (110) one, while another two atoms belong to the inner-core region. Moreover, to treat carefully such localized states on the TiO_2 (110) surface with O vacancies, the on-site d−d Coulomb repulsion term should be included in calculations.[33] We have performed this type of calculations where the effective on-site exchange interaction parameter was kept close to zero and the effective on-site Coulomb interaction parameter was varied from 4.5 to 6.5, as suggested in ref 33. The GGA+U approach has provided the same band dispersion without any shift of the flat bands (not shown here) as in the case of the GGA calculations. Taking into account that our structural model of TiO_2 NWs preserves the TiO_2 stoichiometry without O surface vacancies and our GGA+U calculations reveal no shift in the position of the bands with very small dispersion in addition to the absence of the separate bands in the surface band structure of the TiO_2 (001) surface,[25] our idea to ascribe the origin of these flat and separate bands to surface effects does not hold. It is quite possible that such flat bands stem from bulk. In fact, the band structure of TiO_2 bulk in the rutile phase (Figure 5) displays rather small dispersion for the first conduction band in the Γ-M segment. At the same time, the Γ-M segment

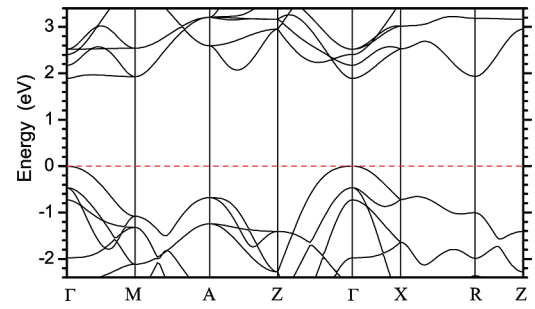

Figure 5. The band structure of bulk TiO_2 in the rutile phase along some symmetry directions of the Brillouin zone (see Figure 6), as calculated by USPP. Zero at the energy scale corresponds to the Fermi energy.

coincides with the [110] direction (see the corresponding Brillouin zone in Figure 6) and with the axis of the ⟨110⟩-oriented TiO_2 NWs transferring its band dispersion to such NWs. In addition, the band structure of the rutile TiO_2 (001) surface shows the first conduction band to have small dispersion along Γ-M.[25] As far as TiO_2 NWs with the ⟨110⟩ axis possess the orthorhombic symmetry, but not the tetragonal one like in bulk, the band degeneracy is removed leading to the splitting of these flat bands. Now it is also clear why these flat bands do not appear in TiO_2 NWs with the ⟨001⟩ orientation: the Γ-Z, M-A and X-R segments do not display small dispersion both in the last valence band and in the first conduction band (Figure 5).

It is also interesting to check changes in band dispersion near the gap region with respect to different morphology. Thus, in the case of the ⟨001⟩-oriented TiO_2 NWs by moving from the rhomb to the polyhedron and, eventually, to the square morphology (the corresponding NWs are shown in the top panel of Figure 1) a progressive band gap reduction is evident (see the top panel of Figure 7). Such a band gap reduction is caused by several top valence bands and bottom conduction bands which are shifted toward each other. O and Ti atoms whose the p and d states respectively populate the top of the valence band

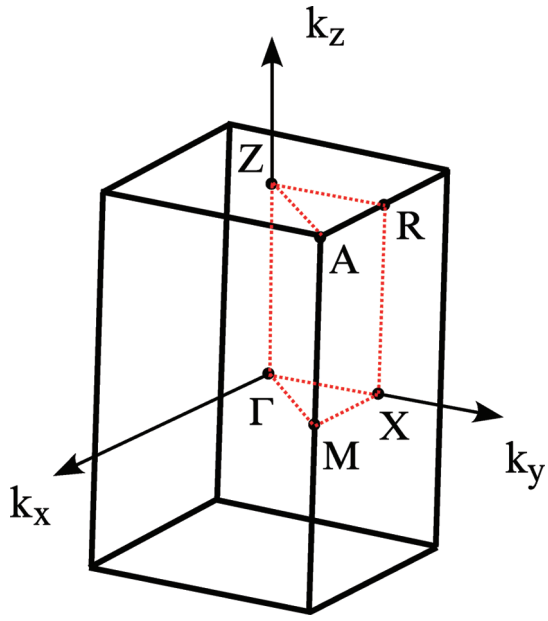

Figure 6. The simple tetragonal Brillouin zone.

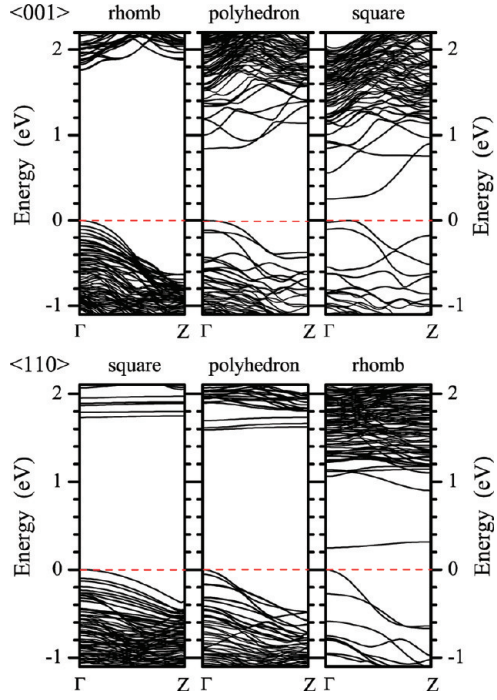

Figure 7. The band structures of TiO_2 NWs as calculated by USPP. (Top panel) The ⟨001⟩-oriented NWs with different morphology shown in the top panel of Figure 1; (Bottom panel) The ⟨110⟩-oriented TiO_2 NWs with different morphology shown in the bottom panel of Figure 1. Zero at the energy scale corresponds to the Fermi energy.

and the bottom of the conduction band of TiO_2 NWs with different morphology are highlighted in Figure 8. In the case of the rhomb morphology, almost all O atoms and one-third of Ti atoms contribute their states to the band extrema, as we have already stated above. For the polyhedron morphology, only some Ti and O surface atoms as well as some O atoms close to the surface of the {110} facets can be spotted. A single Ti surface atom and a few O surface atoms at the {110} facets are identified in the case of the square morphology. To assess possible surface effects, the band structures of the TiO_2 (110) and (100) surfaces have been also calculated and they do not show any sign of similar shifted bands across the gap, as can be seen in Figure

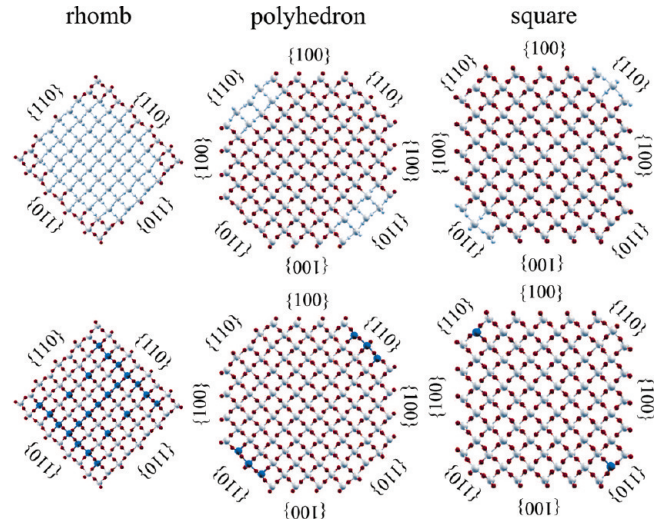

Figure 8. Cross sections of the ⟨001⟩-oriented TiO_2 NW with the different morphology and diameter of 3.9 nm highlighting O (small, light-blue balls) and Ti (large, dark-blue balls) atoms whose states characterized the top valence bands (top panel) and the bottom conduction bands (bottom panel). The rest of the Ti and O atoms are large, light-blue (gray) and small, red (dark) balls, respectively. All facets are indicated.

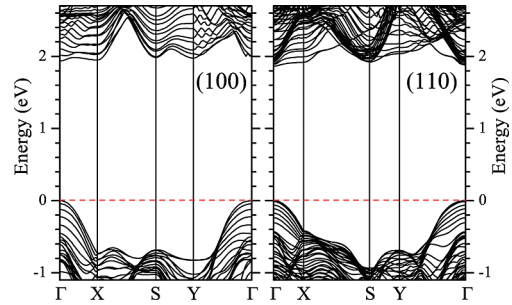

Figure 9. The band structures of the TiO_2 (100) and (110) surfaces. Zero at the energy scale corresponds to the Fermi energy.

9. Therefore, the appearance of the shifted bands in TiO_2 NWs can be attributed to an interaction between edges of the adjacent {110} and {100} facets. This statement seems to be reasonable because the interaction between edges of the adjacent {110} facets does not lead to the shifted bands (the rhomb morphology, see Figure 3) and TiO_2 (110) and (100) surfaces are not characterized by shifted bands either. In addition, we have revealed that both band dispersion and the gaps are invariable and independent of diameter of the polyhedron and of the square NWs (not shown here), as in the case of the rhomb NWs.

The bottom panel of Figure 7 demonstrates the band structures of the ⟨110⟩-oriented TiO_2 NWs with different morphology (the corresponding NWs are shown in the bottom panel of Figure 1). The band structure of the polyhedron NW resembles the one of the square NW except for the smaller number of the flat bands and a slight decreasing in the gaps. However, the band diagram of the rhomb NW displays the sizable band gap reduction. The latter issue occurs because several top valence bands, which are mainly composed of the p states of O surface atoms, shift up in energy in addition to only one flat band located close to the top of the valence band. We have identified Ti atoms whose the d states characterize this flat band and they are indicated in Figure 10. For a representation reason, we have chosen the smallest rhomb TiO_2 NW with the ⟨110⟩ axis in 10 since it possesses the same band dispersion and the gaps as the one with the largest diameter. In addition, the GGA+U

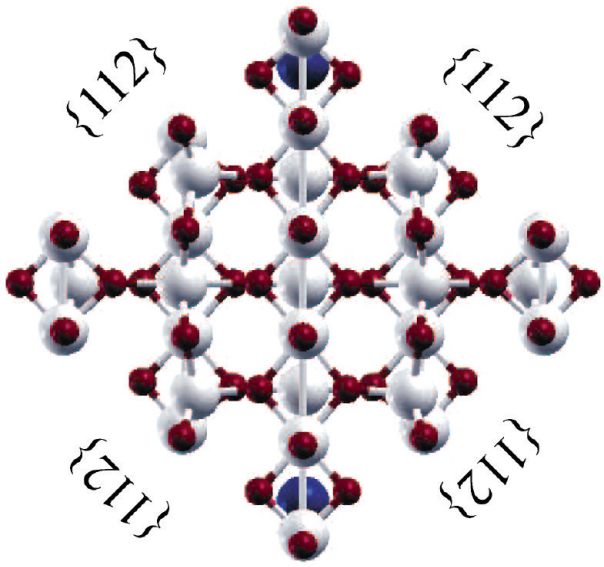

Figure 10. The cross section of the ⟨110⟩-oriented TiO_2 NW with the rhomb morphology and diameter of 1.4 nm. The small, red (dark) balls represent O atoms. The large, light-blue (gray) balls stand for Ti atoms while the large, dark-blue (black) balls indicate Ti atoms whose states form the localized band near the gap region in Figure 7. All facets are indicated.

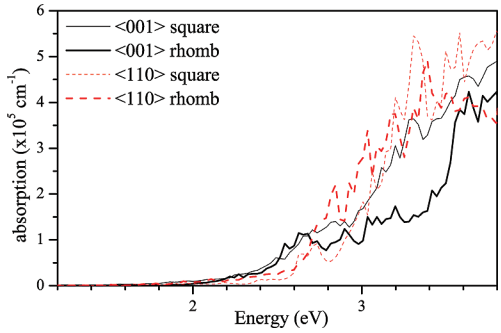

Figure 11. The absorption coefficients of different TiO_2 NWs versus photon energy in the energy range near the gap region.

calculations have revealed no noticeable change in the position of this flat band.

We are aware that our calculations have not been performed within the GW approximation and all band gaps are underestimated. That is why we have deliberately avoided stressing on the calculated gap values in our discussion. However, one more point should be highlighted here. Our results indicate that TiO_2 bulk, the most stable TiO_2 NWs and the TiO_2 (110) and TiO_2 (100) surfaces display almost the same band gap values (see Figures 3, 5, and 9). To this end, we believe that the observed trends in dispersion and in the band gaps are qualitatively correct.

A possibility to sizably shrink the band gaps in TiO_2 NWs by modifying their morphology has been demonstrated in Figure 7. The band gap reduction in TiO_2 NWs with respect to bulk is a feasible way to absorb visible light and increase efficiency of photovoltaic and photocatalytic cells. In this case, it is probably sufficient to treat grown TiO_2 NWs with hot sulfuric acid[17] to change their morphology and, eventually, to tune their band gaps. However, the calculated absorption coefficients for TiO_2 NWs with different morphology and orientations do not show the absorption edge to be shifted to the lower energy range for NWs with smaller gaps (Figure 11). This fact also indicates that oscillator strength of the first direct transitions is rather low,

TABLE 1: Components of the Effective-Mass Tensor for Holes and Electrons in the ⟨001⟩-Oriented TiO_2 NW with the Rhomb Morphology and the ⟨110⟩-Oriented TiO_2 NW with the Square Morphology with Respect to the Ones in Bulk Expressed in Units of Free-Electron Mass

	NWs		bulk	
	⟨001⟩	⟨110⟩	m_{xx}	m_{zz}
holes	5.51	0.83	2.15	3.37
electrons	1.00	12.52	1.14	0.56

while the increase in the values of the absorption coefficients can be attributed to the joint density of interband states. The low oscillator strength occurs because the top of the valence band is composed of the O-p states and the bottom of the conduction band is found to be Ti-d in character, whereas the contributions to the matrix elements come only from on-site transitions.[34] In the calculations of the absorption coefficients for TiO_2 NWs, the local-field effects are not included and we have presented this optical function for the light polarization parallel to the NW axis because it is not suppressed by the depolarization effects.[35] However, in the case of interacting NWs (they are rather close to each other) one can expect the depolarization effects to be not so pronounced, as observed for silicon NWs.[36]

Another factor, which also affects performance of photovoltaic and photocatalytic cells, is charge separation. Electrons and holes generated under the sun's irradiation should be efficiently separated to avoid their recombination indicating that a material should have good transport properties. The effective masses of charge carriers can be used as an indicator of the mobility of the carriers. The estimated effective masses of holes and electrons for the ⟨001⟩-oriented TiO_2 NWs with the rhomb morphology and the ⟨110⟩-oriented TiO_2 NWs with the square morphology are summarized in Table 1. It is evident that they have turned out to be relatively large, however, being quite comparable to the ones of TiO_2 bulk calculated in the Γ point.

Conclusions

Our ab initio calculations clearly demonstrate that the most thermodynamically preferable TiO_2 NWs in the rutile phase without hydrogen passivation and O vacancies display the {110} facets in the case of their ⟨001⟩ orientation and the {110} and {001} facets in the case of their ⟨110⟩ orientation. We have also shown morphology to affect stability of TiO_2 NWs at small diameters, while at larger diameters its role is attenuated. The most stable ⟨001⟩-oriented TiO_2 NWs are characterized by the band gap values that are invariable with respect to diameter of the nanostructures and close to the one of bulk. Such band gap behavior is anomalous with respect to expected changes in gap values due to quantum confinement effects. This happens because of the stabilization role of the states in the top valence bands and in the bottom conduction bands that come from atoms located close to and at the surface of these nanostructures. We have also suggested that the interaction between edges of the adjacent {110} and {100} facets in TiO_2 NWs with the ⟨001⟩ axis leads to the sizable band gap reduction. In the case of the ⟨110⟩-oriented TiO_2 NWs, the presence of the flat bands like localized levels in the gap region is found to be the intrinsic feature of such nanostructures, which is not connected with O vacancies or surface states. These flat bands composed of Ti-d states also provide a decrease in the band gaps. The presented band structures of different TiO_2 NWs do not show any sign of surface dangling bonds in the gap region indicating that the H

passivation is not appropriate for these nanostructures. The absorption coefficients for TiO_2 NWs with different morphology and orientations do not follow changes in the gaps and do not display any shift of the absorption edge to the lower energy range. The ⟨001⟩-oriented TiO_2 NWs with the rhomb morphology can be considered as a suitable material for photovoltaic and photocatalytic cells, however an efficient way to shift the absorption edge to the lower energy range and to improve transport properties of these NWs should be found.

Acknowledgment. The authors thank Drs. A. B. Filonov and N. N. Dorozhkin for their fruitful discussion, useful suggestions, and comments on the results presented in the paper. This work has been supported by Belarusian Republican Foundation for Fundamental Research under Grant T09F-004.

References and Notes

(1) Diebold, U. *Surf. Sci. Rep.* **2003**, *48*, 53.
(2) Chen, X.; Mao, S. S. *Chem. Rev.* **2007**, *107*, 2891.
(3) Qi, Q.; Zhang, T.; Wang, L. *Appl. Phys. Lett.* **2008**, *93*, 023105.
(4) Wu, J.-J.; Chen, G.-R.; Lu, C.-C.; Wu, W.-T.; Chen, J.-S. *Nanotechnology* **2008**, *19*, 105702.
(5) Wu, J.-M.; Shih, H.; Tseng, Y.-K.; Hsu, C.-L.; Tsay, C.-Y. *J. Electrochem. Soc.* **2007**, *154*, H157.
(6) Sciancalepore, C.; Cassano, T.; Curri, M. L.; Mecerreyes, D.; Valentini, A.; Agostiano, A.; Tommasi, R.; Striccoli, M. *Nanotechnology* **2008**, *19*, 205705.
(7) Baik, J. M.; Kim, M. H.; Larson, C.; Chen, X.; Guo, S.; Wodtke, A. M.; Moskovits, M. *Appl. Phys. Lett.* **2008**, *92*, 242111.
(8) Wu, J.-M.; Shih, H. C.; Wu, W.-T. *Chem. Phys. Lett.* **2005**, *413*, 490.
(9) Wu, J.-M.; Shih, H. C.; Wu, W.-T. *Nanotechnology* **2006**, *17*, 105.
(10) Lee, J.-C.; Park, K.-S.; Kim, T.-G.; Choi, H.-J.; Sung, Y.-M. *Nanotechnology* **2006**, *17*, 4317.
(11) Amin, S. S.; Nicholls, A.; Xu, T. T. *Nanotechnology* **2007**, *18*, 445609.
(12) Chen, C. A.; Chen, Y. M.; Korotcov, A.; Huang, Y. S.; Tsai, D. S.; Tiong, K. K. *Nanotechnology* **2007**, *19*, 075611.
(13) Peng, H.; Li, J. *J. Phys. Chem. C* **2008**, *112*, 20241.
(14) Ramamoorthy, M.; Vanderbilt, D.; King-Smith, R. D. *Phys. Rev. B* **1994**, *49*, 16721.
(15) Perron, H.; Domain, C.; Roques, J.; Drot, R.; Simoni, E.; Catalette, H. *Theor. Chem. Acc.* **2007**, *117*, 565.
(16) Pang, C. L.; Thornton, G. *Surf. Sci.* **2006**, *600*, 4405.
(17) Taguchi, T.; Saito, Y.; Sarukawa, K.; Ohno, T.; Matsumura, M. *New J. Chem.* **2003**, *27*, 1304.
(18) Migas, D. B.; Borisenko, V. E. *J. Appl. Phys.* **2009**, *105*, 104316.
(19) Kresse, G.; Hafner, J. *Phys. Rev. B* **1994**, *49*, 14251.
(20) Kresse, G.; Furthmüller, J. *Comput. Mater. Sci.* **1996**, *6*, 15.
(21) Kresse, G.; Furthmüller, J. *Phys. Rev. B* **1996**, *54*, 11169.
(22) Perdew, J. P.; Chevary, J. A.; Vosko, S. H.; Jackson, K. A.; Pederson, M. R.; Singh, D. J.; Fiolhais, C. *Phys. Rev. B* **1992**, *46*, 6671.
(23) Liechtenstein, A. I.; Anisimov, V. I.; Zaane, J. *Phys. Rev. B* **1995**, *52*, R5467.
(24) Blaha, P.; Schwarz, K.; Madsen, G. K. H.; Kvasnicka, D.; Luitz, J. *WIEN2k, An Augmented Plane Wave + Local Orbitals Program for Calculating Crystal Properties*; Karlheinz Schwarz, Techn. UniversitatWien: Austria, 2001. ISBN 3-9501031-1-2.
(25) Hua, Z.; Songyuan, D.; Kongjia, W. *Plasma Sci. Technol.* **2004**, *6*, 2467.
(26) Thompson, S. J.; Lewis, S. P. *Phys. Rev. B* **2006**, *73*, 073403.
(27) Wang, C. X.; Wang, B.; Yang, Y. H.; Yang, G. W. *J. Phys. Chem. B* **2005**, *109*, 9966.
(28) Liu, Q. X.; Wang, C. X.; Xu, N. S.; Yang, G. W. *Phys. Rev. B* **2005**, *72*, 085417.
(29) Zhao, X.; Wei, C. M.; Yang, L.; Chou, M. Y. *Phys. Rev. Lett.* **2004**, *92*, 236805.
(30) Migas, D. B. *J. Appl. Phys.* **2005**, *98*, 054310.
(31) Monticone, S.; Tufeu, R.; Kanaev, A. V.; Scolan, E.; Sanchez, C. *Appl. Surf. Sci.* **2000**, *162−163*, 565.
(32) Serpone, N.; Laeless, D.; Khairutdinov, R. *J. Phys. Chem.* **1995**, *99*, 16646.
(33) Calzado, C.; Hernandez, N.; Sanz, J. *Phys. Rev. B* **2008**, *77*, 045118.
(34) Migas, D. B.; Miglio, L.; Henrion, W.; Rebien, M.; Marabelli, F.; Cook, B. A.; Shaposhnikov, V. L.; Borisenko, V. E. *Phys. Rev. B* **2001**, *64*, 075208.
(35) Bruneval, F.; Botti, S.; Reining, L. *Phys. Rev. Lett.* **2005**, *94*, 219701.
(36) Bruno, M.; Palummo, M.; Sole, R. D.; Ossicini, S. *Phys. Rev. Lett.* **2007**, *98*, 036807.

JP106117Y